

Inverse Kinetic Isotope Effect in the Excited-State Relaxation of a Ru(II)–Aquo Complex: Revealing the Impact of Hydrogen-Bond Dynamics on Nonradiative Decay

Joshua T. Hewitt,[†] Javier J. Concepcion,[‡] and Niels H. Damrauer^{*,†}

[†]Department of Chemistry and Biochemistry, University of Colorado, Boulder, Colorado 80309, United States

[‡]Department of Chemistry, The University of North Carolina, Chapel Hill, North Carolina 27599-3290, United States

S Supporting Information

ABSTRACT: Photophysics of the MLCT excited-state of $[\text{Ru}(\text{bpy})(\text{tpy})(\text{OH}_2)]^{2+}$ (**1**) and $[\text{Ru}(\text{bpy})(\text{tpy})(\text{OD}_2)]^{2+}$ (**2**) (bpy = 2,2'-bipyridine and tpy = 2,2':6',2''-terpyridine) have been investigated in room-temperature H_2O and D_2O using ultrafast transient pump-probe spectroscopy. An inverse isotope effect is observed in the ground-state recovery for the two complexes. These data indicate control of excited-state lifetime via a pre-equilibrium between the $^3\text{MLCT}$ state that initiates H-bond dynamics with the solvent and the ^3MC state that serves as the principal pathway for nonradiative decay.

Sustainable conversion of sunlight to chemical fuels demands molecules and materials that can negotiate light absorption, charge separation, energy storage, and multi-electron/proton redox chemistry. At this stage it is critical that species with promising functionality be characterized under visible light excitation conditions in aqueous solvent to assess their potential role in energy conversion and to guide future modifications. Mononuclear Ru(II) metal-aquo complexes have been scrutinized as electrochemical water oxidation catalysts with $[\text{Ru}(\text{bpy})(\text{tpy})(\text{OH}_2)]^{2+}$ and derivatives receiving attention.^{1–7} In the Ru(II) oxidation state, complexes of this nature are highly colored by their metal-to-ligand charge transfer (MLCT) band,^{7–9} and one can imagine their participation, by design or as an unintended consequence of their absorption features, in light harvesting and redox photochemistry. A characterization of dynamics within the MLCT manifold, including the influence of proton-motion coordinates,^{10–14} is required and is the subject of this current work.

The visible absorption spectrum of $[\text{Ru}(\text{bpy})(\text{tpy})(\text{OH}_2)]^{2+}$ dissolved in H_2O (**1**) (or $[\text{Ru}(\text{bpy})(\text{tpy})(\text{OD}_2)]^{2+}$ dissolved in D_2O (**2**)) is dominated by an intense $^1\text{MLCT} \leftarrow ^1\text{GS}$ absorption feature (Figure 1; $\epsilon_{480 \text{ nm}} = 9600 \text{ M}^{-1}\text{cm}^{-1}$) which serves as the access point for our investigation of the charge-transfer excited-state photophysics in this complex.^{1,15} These compounds are very weakly emissive at room temperature,¹⁵ and we have relied on ultrafast pump-probe experiments to characterize their photophysics. The transient absorption (TA) features observed in the chirp-corrected magic angle spectra (see Supporting Information (SI) for experimental details) collected at $\Delta t = 2$ and 100 ps after excitation with pump pulses centered at 495 nm (Figure 1 for **1**; Figure S1 for **2**) clearly establish that we are

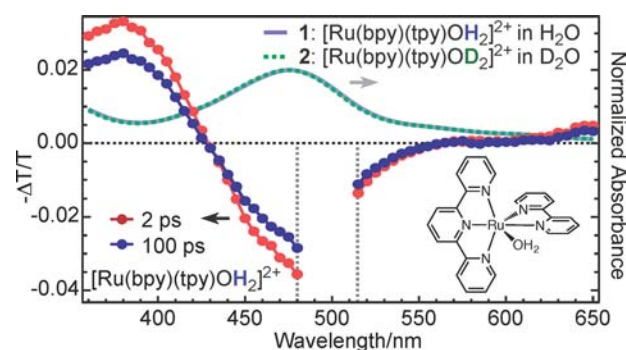


Figure 1. Right axis: Ground-state (GS) absorption spectra of **1** and **2** showing insensitivity of GS electronic properties to the isotopic nature of the aqueous solvent. Left axis: TA spectra of **1** at $\Delta t = 2$ and 100 ps showing $^3\text{MLCT}$ character. Data between the dashed vertical lines is omitted due to contamination by pump scatter (495 nm excitation).

observing the $^3\text{MLCT}$ excited state. Most notably, the prominent absorption feature peaked at 390 nm corresponds to reduced tpy ligand $\pi^* \leftarrow \pi^*$ absorption and heralds the tpy-localized $^3\text{MLCT}$ excited state.^{16,17} The weak absorption at 650 nm correlates well with the ground-state absorption spectrum of the oxidized species^{5,18} $[\text{Ru}(\text{bpy})(\text{tpy})(\text{OH}_2)]^{3+}$ and is attributed to LMCT from π orbitals to the hole on the metal center.^{17,19}

Detailed temporal evolution of the $^3\text{MLCT}$ of **1** was monitored by collecting single wavelength kinetics at 400, 470, and 650 nm as seen in Figure 2. While the TA spectra (Figures 1 and S1) were collected with an excitation wavelength of 495 nm, the single wavelength kinetics used pulses centered at 525 nm. Red-detuning minimizes the amplitude of vibrational cooling dynamics²⁰ and favors charge transfer to the low-energy tpy ligand.²¹ Triplicate sets of data collected at each wavelength were globally fit (see SI for details) leading to the observation of a dominant decay of 270 ± 18 ps present at all the probe wavelengths (Table 1). The absorption data at $\lambda_{\text{probe}} = 400$ nm were found to be mono-exponential, while data collected at 470 nm and also at 650 nm (albeit more weakly) have an additional early time component of 2 ± 1 ps (highlighted in Figure 2 inset). Additional spectra probing bluer wavelengths confirm these early time dynamics (Figure S2).

Received: April 15, 2013

Published: August 8, 2013

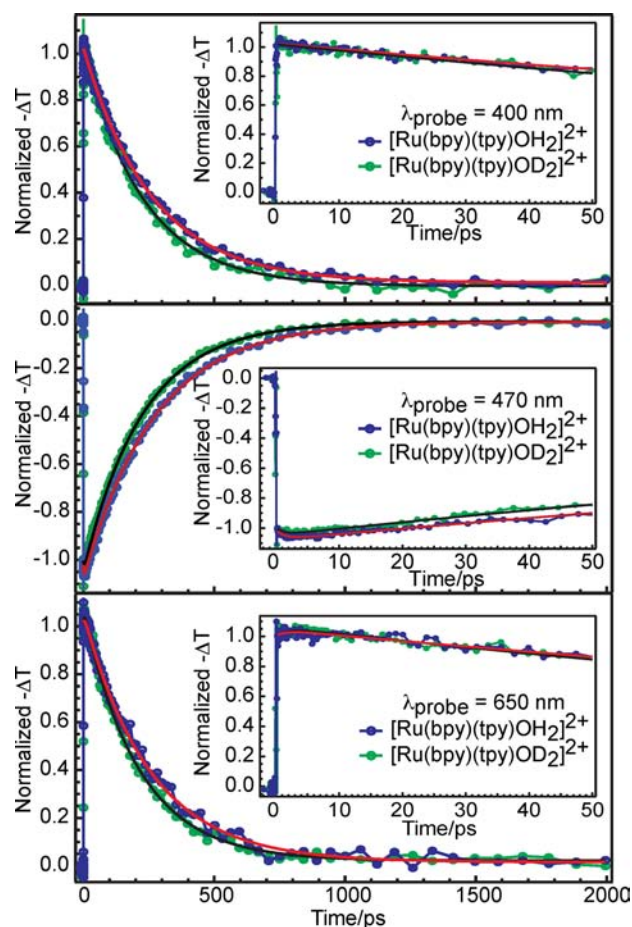


Figure 2. Magic angle kinetics ($\lambda_{\text{probe}} = 400$ nm (top), 470 nm (middle), and 650 nm (bottom); 525 nm excitation) for **1** (blue) and **2** (green) showing evidence for an inverse KIE at all probe wavelengths. Solid lines are the result of a global fit of data collected for each molecule at each probe color (see Table 1).

Table 1. Global Fitting for Data Collected at Room Temperature for **1 and **2****

$\lambda_{\text{probe}}/\text{nm}$		$\tau_1/\text{ps}(2\sigma)$	$A_1(2\sigma)$	$\tau_2/\text{ps}(2\sigma)$	$A_2(2\sigma)$
400	1	270(18)	1.00(0.01)	–	–
	2	220(12)	1.00(0.02)	–	–
470	1	270(18)	–1.00(0.06)	2(1)	0.06(0.02)
	2	220(12)	–1.00(0.02)	1.4(0.5)	0.05(0.02)
650	1	270(18)	1.10(0.06)	2(1)	–0.03(0.06)
	2	220(12)	0.99(0.06)	1.4(0.5)	–0.03(0.04)

A brief discussion of the 2 ps decay component will follow. Here we note that the dominant 270 ps recovery of the ground state is comparable to the 250 ps lifetime reported for $[\text{Ru}(\text{tpy})_2]^{2+}$ in neat water.¹⁶ Broadly speaking, the $^3\text{MLCT}$ excited state in both complexes are similar, with a reduced tpy ligand proximal to a formal Ru(III) metal center. Both systems have weak ligand fields compared to the tris-analogue $[\text{Ru}(\text{bpy})_3]^{2+}$ due to the hindered bite angle of the tpy ligand^{22,23} causing the $^3\text{MLCT}$ manifold to be energetically proximal to triplet ligand field excited states (^3MC). This is supported in computational work by Jakubikova et al. regarding **1** that includes treatment of explicit water solvation effects.¹⁵ There are two simplified excited-state decay pictures which can explain the short 270 ps ground-state recovery while observing $^3\text{MLCT}$

character in the TA spectra, both of which are based on the following reaction (eq 1) for loss of the $^3\text{MLCT}$ state (these ignore the slower²⁴ direct $^3\text{MLCT}$ to ^1GS interconversion commonly tied to the rate constant k_0).



In the first, $k_2 \gg k_1$ and k_{-1} and thermal activation to the ^3MC would rate limit ground-state recovery. The second involves a pre-equilibrium between the $^3\text{MLCT}$ and ^3MC ²⁵ (i.e., $(k_1 + k_{-1}) \gg k_2$) such that ground-state recovery is rate limited by thermal activation from ^3MC to ^1GS and the overall excited state decay (and ground-state recovery) would have a rate constant $k_{\text{obs}} = (k_1/k_{-1}) \cdot k_2 = K_{\text{eq}} \cdot k_2$. We have recently argued¹⁷ that the second decay mechanism is relevant for $[\text{Ru}(\text{tpy})_2]^{2+}$ based on the observation of additional early time decay dynamics. Given the similar state and energy structure of **1** (and **2**) to $[\text{Ru}(\text{tpy})_2]^{2+}$ as well as the isotope effect discussed below, we expect this second decay mechanism to be most relevant here as well.

A similar suite of pump-probe experiments were performed on the isotopologue **2**. We note that the labile nature of the aquo ligands precludes conducting experiments with a deuterated ligand and a protiated solvent or vice versa (see SI for detail). The TA spectrum of **2** collected at 100 ps after excitation (Figure S3) overlays closely with that of **1**. Temporal evolution of the $^3\text{MLCT}$ in **2** was also monitored via single wavelength kinetics at 400, 470, and 650 nm (Figure 2). As was seen for the H₂O data, global fitting of triplicate sets of D₂O data reveals a dominant longer decay component at all wavelengths and a weak, faster component at 470 nm and at 650 nm (Table 1).

Most striking is the shortening of the observed lifetime $\tau_{\text{obs}} = 1/k_{\text{obs}} = 220$ ps for the D₂O isotopologue to be compared with the 270 ps measured for **1**. This indicates the presence of an inverse kinetic isotope effect (KIE) where the ratio of observed rate constants in H₂O versus D₂O is 0.81. It is emphasized that the ground-state absorption spectra of the two isotopologues are superimposable (Figure 1) signifying no obvious changes in Franck–Condon state energetics that might explain the inverse KIE.

It is noted that normal KIEs have been observed in the nonradiative decay of related d⁶ metal polypyridyl systems^{26–28} including $[\text{M}(\text{bpy})_3]^{2+}$ and $[\text{M}(\text{phen})_3]^{2+}$ (where, M = Ru and Os) solvated in H₂O versus D₂O. These have been ascribed to quantum mechanical effects involving overtones of high-frequency solvent O–H(D) vibrations acting as energy-transfer acceptors and where a higher overtone is needed for D₂O.^{28,29} For completeness, we have looked at the analogous Ru(II) complex, $[\text{Ru}(\text{tpy})_2]^{2+}$, which has an excited-state lifetime comparable to **1** and **2** but obviously no bound aquo ligand. Compared to **1**, $[\text{Ru}(\text{tpy})_2]^{2+}$ stores a very similar amount of excited-state energy in the $^3\text{MLCT}$ state based on nearly identical emission maxima measured in room-temperature water.¹⁵ Our study was not exhaustive, and we report only bleach recovery dynamics collected in H₂O and in D₂O at 470 nm (Figure S4) where fitting reveals a normal, albeit weak, KIE ($\tau_{\text{obs H}_2\text{O}} = 234 \pm 4$ ps; $\tau_{\text{obs D}_2\text{O}} = 254 \pm 5$ ps). Its weakness compared to related tris-complexes is presumed to be a result of the higher rate of nonradiative decay which competes more effectively against resonance energy transfer to O–H or O–D solvent overtones. These observations in $[\text{Ru}(\text{tpy})_2]^{2+}$ argue against an explanation for the inverse KIE in **1** and **2** involving energy transfer to solvent overtones via either the $^3\text{MLCT}$ or the energetically proximal

^3MC which have been calculated in **1**, with inclusion of explicit water molecules, to be 2 kcal/mol lower in energy.¹⁵

To explain the inverse KIE seen here, one could possibly invoke differences in electronic coupling between states involved in the rate limiting of ground-state recovery (^3MC and ^1GS for the second mechanism discussed above). Such an argument would presumably need to take advantage of known differences in spectral densities between H_2O and D_2O for higher-frequency librational motions and/or stretching motions.³⁰ However, the fact that the KIE's seen for $[\text{Ru}(\text{tpy})_2]^{2+}$ versus the aquo complexes oppose each other argues against this explanation or at the very least, significantly raises the bar in explaining the source of a frequency-dependent electronic state coupling. It is noted that Hammes-Schiffer et al. have recently used new theoretical tools to show that a weak inverse KIE can manifest in ultrafast highly exergonic proton-coupled electron-transfer (PCET) reactions due to changes in vibronic coupling.³¹ While, a direct $^3\text{MLCT} \rightarrow ^1\text{GS}$ conversion may be expected to have PCET character (given increased proton-donor ability of the aquo-ligand in the $^3\text{MLCT}$, *vide infra*), the fact that the ^3MC kinetically controls ground-state recovery leads us to believe that such mechanisms are not at play in our observations.

In the context of eq 1, an inverse KIE for ground-state recovery would manifest if the pre-equilibrium shown preferentially shifted toward the $^3\text{MLCT}$ state in H_2O compared to D_2O . It is possible to rule out electrostatic (Born) effects causing this for two reasons. First, the room-temperature dielectric constants for H_2O and D_2O as well as the coefficients that determine their temperature dependence are nearly identical.³² Second, in contrast to the experimental observation, one would again expect the sign of the KIE to be the same as that seen for $[\text{Ru}(\text{tpy})_2]^{2+}$. The appropriate shifting of this equilibrium constant can, on the other hand, be understood in the context of solvent isotope effects on transition-metal coordination complex redox potentials as well as electron-transfer (ET) cross reactions. In particular, we point to work by Weaver et al.³³ who showed, using a wide range of compounds, that $n + 1/n$ couples (e.g., $3+/2+$) of metal complexes containing aquo ligands exhibit large positive shifts on transferring from H_2O to D_2O . For example, $E_{1/2}$ (versus SCE) is 495 mV for $[\text{Fe}(\text{H}_2\text{O})_6]^{3+/2+}$ while 538 mV for $[\text{Fe}(\text{D}_2\text{O})_6]^{3+/2+}$. In terms of one-electron reduction half reactions, this means that the oxidized form of the complex is more stable in H_2O than it is in D_2O . Such effects are born out in numerous ET cross reactions such as between $[\text{Co}(\text{NH}_3)_6]^{3+}$ and aqueous Cr^{2+} ions where the ratio of equilibrium constants in H_2O versus D_2O is of order ten³³ (i.e., the reaction proceeds further toward the oxidized form of the aqueous ion in H_2O than it does in D_2O). When, on the other hand, the coordination sphere of the metal complex is saturated by ligands that do not engage in hydrogen bonding with the solvent, these couples are largely invariant to aqueous solvent isotope changes.³³

There is, of course, no formal ET reaction in the equilibrium shown in eq 1. However, with respect to the ruthenium center proximal to the water ligand and its H-bonding network, the conversion from ^3MC to $^3\text{MLCT}$ represents a formal change in oxidation state from $2+$ to $3+$. Therein, we expect the $^3\text{MLCT}$ to be preferentially stabilized for **1** compared to **2**. Given that ground-state recovery proceeds via the ^3MC reaction channel, this will manifest in the observation of an inverse KIE.

We emphasize, in analogy to Weaver's work, that the aquo ligand is an essential component to our observation. As the formal oxidation state of the ruthenium center shifts from $2+$

(^3MC) to $3+$ ($^3\text{MLCT}$), the force constant for stretching within the bound H_2O or D_2O will decrease due to increased electron donation to the metal center.³⁴ As well, this force constant in proximal solvent molecules will decrease as the oxygen atoms become more engaged in H(D) bonding.³⁵ This means that the zero-point energy difference between **1** and **2** is expected to be larger in the ^3MC state (where the force constant for stretching in the aquo ligand is larger) than in the $^3\text{MLCT}$ state (where it is smaller). In enthalpic terms, then, there would be a relative shift in the pre-equilibrium toward the $^3\text{MLCT}$ from the ^3MC in H_2O versus D_2O (see TOC graphic). Entropic terms are also expected to be at play.^{31,36} As the $^3\text{MLCT}$ is formed in either **1** or **2**, the acidity of the aquo ligand increases, which would initiate the formation of more H-bonding structure within proximal solvent environs. Considering that D_2O is known to engage in hydrogen bonding with other solvent molecules to a larger degree than its lighter isotopologues,³⁷ it stands to reason that a more ordered solvent environment would arise for the $^3\text{MLCT}$ state in **2** compared to **1**. Thus an entropic contribution would act to shift the pre-equilibrium toward the ^3MC for **2** relative to **1**. Preliminary temperature-dependent studies indicate a constant inverse KIE over the range 277–343 K. This suggests that entropic contributions are important and that more detailed explorations are warranted.

We return to a discussion of the weak short time-scale (~ 2 ps) decay components observed at 470 and 650 nm in **1** and **2**. While an inverse KIE is also seemingly apparent (Table 1), the fit uncertainty and the convolution of dynamics with the establishment of the $^3\text{MLCT} \leftrightarrow ^3\text{MC}$ equilibrium (*vide supra*) precludes a meaningful interpretation at this time. A more detailed study of the evolution of spectra will likely be needed. We wish to focus here on whether the observed ~ 2 ps features are consistent with the photophysical picture that has been put forth. First, we rule out vibrational cooling²⁰ and interligand ET¹⁷ ($\text{bpy}^{\bullet-} \rightarrow \text{tpy}$) within the $^3\text{MLCT}$ manifold as the source. For both processes one would expect growth of absorption intensity at 400 nm, in contrast to our observations. A scenario that is consistent involves shifting of LMCT absorption features in response to the H-bond dynamics discussed above. Berlinguette et al.⁵ and Sakai et al.¹⁸ have measured the absorption spectrum of the one-electron oxidized $[\text{Ru}(\text{bpy})(\text{tpy})(\text{OH}_2)]^{3+}$ in H_2O . Their data show evidence for two LMCT features that would be present in the spectral window of our TA experiment. The first is a weak, broad absorption centered near 700 nm attributable to LMCT originating from the tpy ligand.¹⁷ The second is the tail of a relatively stronger absorption extending from 350 to ~ 500 nm assigned to LMCT transitions involving the bpy ligand.¹⁸

As noted above, these LMCT transitions involve promotion of an electron from a ligand π orbital to the hole in the metal center $d\pi$ orbitals. Concomitant with partial proton donation to solvent by the aquo ligand within the $^3\text{MLCT}$ state, hydroxyl character will develop in the coordination sphere of the metal. Given its π -donor character, such a ligand environment is expected to raise the energy of the metal $d\pi$ orbitals leading to LMCT blue shifting. Consistent with these predictions, we observe a slight increase in absorption at 650 nm that may be ascribed to blue shifting of the tpy-based LMCT as hydroxyl character develops on a 2 ps time scale. It is interesting to note that this time scale matches well with the orientational relaxation time of liquid water determined by both theory^{38,39} and experiment.^{40–42} As well the magnitude of the bleach at 470 nm increases. This can only occur if the total signal that is interrogated includes absorptive components (i.e., is not exclusively bleach in nature)

and that these components decrease in intensity as the system evolves. Here the transient blue shifting of the higher energy bpy-based LMCT (vide supra) helps to explain the observation. Based on this same discussion, one might also predict that early time picosecond rise dynamics should be observed in the 400 nm absorption feature in contrast to our observation. This absence of dynamics can be accounted for by also considering the spectral intensity changes associated with equilibration between the ³MLCT and ³MC states (vide supra). We have shown previously in [Ru(tpy)₂]²⁺ that the hallmark of such equilibration is loss of reduced ligand absorption at early times without concomitant recovery of the bleach.¹⁷ For **1** and **2** such dynamics would include a transient decrease in intensity of the absorption feature centered at 380 nm⁴³ which in turn would offset the rise at 400 nm that is expected from the blue shifting of the bpy-based LMCT. Thus, overlapping and offsetting spectral changes associated with proton motion of the coordinated aquo ligand and ³MLCT-³MC equilibration may explain the absence of observed early time dynamics at 400 nm.

In summary, ultrafast TA spectroscopy has been used to probe the MLCT reactivity of **1** and **2** in room-temperature H₂O and D₂O, respectively. The observation of an inverse KIE highlights the mechanistic importance of the water molecule in the coordination sphere of the metal in determining excited-state properties. It suggests fast H-bond dynamics initiated from the ³MLCT state having Ru(III) character, which competes with facile recovery of the ground state via population of the ³MC (with Ru(II) character). Partial proton motion and the response of the solvent preserves MLCT electronic character while simultaneously increasing the time available to engage in redox chemistry and/or oxygen-activation chemistry. Provided that excited-state energies are carefully managed, architectures exploiting endogenous or exogenous basic sites, above and beyond the solvent, may have enhanced ability to direct useful photochemistry.

■ ASSOCIATED CONTENT

📄 Supporting Information

Experimental details and characterization data. This material is available free of charge via the Internet at <http://pubs.acs.org>.

■ AUTHOR INFORMATION

Corresponding Author

Niels.Damrauer@Colorado.edu

Notes

The authors declare no competing financial interest.

■ ACKNOWLEDGMENTS

We gratefully acknowledge financial support for this work from the National Science Foundation award no. 0847216 and from an Alfred P. Sloan Research Fellowship and thank Prof. T.J. Meyer of UNC Chapel Hill for useful discussions.

■ REFERENCES

- (1) Takeuchi, K. J.; Thompson, M. S.; Pipes, D. W.; Meyer, T. J. *Inorg. Chem.* **1984**, *23*, 1845.
- (2) Tseng, H. W.; Zong, R.; Muckerman, J. T.; Thummel, R. *Inorg. Chem.* **2008**, *47*, 11763.
- (3) Deng, Z. P.; Tseng, H. W.; Zong, R. F.; Wang, D.; Thummel, R. *Inorg. Chem.* **2008**, *47*, 1835.
- (4) Concepcion, J. J.; Jurs, J. W.; Templeton, J. L.; Meyer, T. J. *J. Am. Chem. Soc.* **2008**, *130*, 16462.

- (5) Wasylenko, D. J.; Ganesamoorthy, C.; Henderson, M. A.; Koivisto, B. D.; Osthoff, H. D.; Berlinguette, C. P. *J. Am. Chem. Soc.* **2010**, *132*, 16094.
- (6) Duan, L. L.; Araujo, C. M.; Ahlquist, M. S. G.; Sun, L. C. *Proc. Natl. Acad. Sci. U.S.A.* **2012**, *109*, 15584.
- (7) Tseng, H.-W.; Wilker, M. B.; Damrauer, N. H.; Dukovic, G. *J. Am. Chem. Soc.* **2013**, *135*, 3383.
- (8) Kaveevitichai, N.; Chitta, R.; Zong, R. F.; El Ojaimi, M.; Thummel, R. P. *J. Am. Chem. Soc.* **2012**, *134*, 10721.
- (9) Treadway, J. A.; Moss, J. A.; Meyer, T. J. *Inorg. Chem.* **1999**, *38*, 4386.
- (10) Gagliardi, C. J.; Westlake, B. C.; Kent, C. A.; Paul, J. J.; Papanikolas, J. M.; Meyer, T. J. *Coord. Chem. Rev.* **2010**, *254*, 2459.
- (11) Stewart, D. J.; Brennaman, M. K.; Bettis, S. E.; Wang, L.; Binstead, R. A.; Papanikolas, J. M.; Meyer, T. J. *J. Phys. Chem. Lett.* **2011**, *2*, 1844.
- (12) Wenger, O. S. *Chem.—Eur. J.* **2011**, *17*, 11692.
- (13) Pizano, A. A.; Yang, J. L.; Nocera, D. G. *Chem. Sci.* **2012**, *3*, 2457.
- (14) Manner, V. W.; Mayer, J. M. *J. Am. Chem. Soc.* **2009**, *131*, 9874.
- (15) Jakubikova, E.; Chen, W. Z.; Dattelbaum, D. M.; Rein, F. N.; Rocha, R. C.; Martin, R. L.; Batista, E. R. *Inorg. Chem.* **2009**, *48*, 10720.
- (16) Winkler, J. R.; Netz, T. L.; Creutz, C.; Sutin, N. *J. Am. Chem. Soc.* **1987**, *109*, 2381.
- (17) Hewitt, J. T.; Vallett, P. J.; Damrauer, N. H. *J. Phys. Chem. A* **2012**, *116*, 11536.
- (18) Kimoto, A.; Yamauchi, K.; Yoshida, M.; Masaoka, S.; Sakai, K. *Chem. Commun.* **2012**, *48*, 239.
- (19) Zališ, S.; Consani, C.; El Nahhas, A.; Cannizzo, A.; Chergui, M.; Hartl, F.; Vlček, A. *Inorg. Chim. Acta* **2011**, *374*, 578.
- (20) Shaw, G. B.; Styers-Barnett, D. J.; Gannon, E. Z.; Granger, J. C.; Papanikolas, J. M. *J. Phys. Chem. A* **2004**, *108*, 4998.
- (21) Gardner, J. S.; Strommen, D. P.; Szulbinski, W. S.; Su, H. Q.; Kincaid, J. R. *J. Phys. Chem. A* **2003**, *107*, 351.
- (22) Lashgari, K.; Kritikos, M.; Norrestam, R.; Norrby, T. *Acta Crystallogr., Sect. C: Cryst. Struct. Commun.* **1999**, *55*, 64.
- (23) Hammarström, L.; Johansson, O. *Coord. Chem. Rev.* **2010**, *254*, 2546.
- (24) Amini, A.; Harriman, A.; Mayeux, A. *Phys. Chem. Chem. Phys.* **2004**, *6*, 1157.
- (25) Rae, M.; Berberan-Santos, M. N. *J. Chem. Educ.* **2004**, *81*, 436.
- (26) Van Houten, J.; Watts, R. J. *J. Am. Chem. Soc.* **1975**, *97*, 3843.
- (27) Sriram, R.; Hoffman, M. Z. *Chem. Phys. Lett.* **1982**, *85*, 572.
- (28) Masuda, A.; Kaizu, Y. *Inorg. Chem.* **1998**, *37*, 3371.
- (29) Chen, P.; Meyer, T. J. *Chem. Rev.* **1998**, *98*, 1439.
- (30) Max, J. J.; Chapados, C. *J. Chem. Phys.* **2009**, *131*, 184505.
- (31) Hazra, A.; Soudackov, A. V.; Hammes-Schiffer, S. *J. Phys. Chem. Lett.* **2011**, *2*, 36.
- (32) Arnett, E. M.; McKelvey, D. R. In *Solute-Solvent Interactions*; Coetzee, J. F., Ritchie, C. D., Eds.; Marcel Dekker: New York, 1969; p 343.
- (33) Weaver, M. J.; Nettles, S. M. *Inorg. Chem.* **1980**, *19*, 1641.
- (34) Bigeleisen, J. *J. Chem. Phys.* **1960**, *32*, 1583.
- (35) Bunton, C. A.; Shiner, V. J. *J. Am. Chem. Soc.* **1961**, *83*, 42.
- (36) Hupp, J. T.; Weaver, M. J. *Inorg. Chem.* **1984**, *23*, 3639.
- (37) Soper, A. K.; Benmore, C. J. *Phys. Rev. Lett.* **2008**, *101*, 065502.
- (38) Laage, D.; Hynes, J. T. *Science* **2006**, *311*, 832.
- (39) Lawrence, C. P.; Skinner, J. L. *J. Chem. Phys.* **2003**, *118*, 264.
- (40) Nicodemus, R. A.; Corcelli, S. A.; Skinner, J. L.; Tokmakoff, A. *J. Phys. Chem. B* **2011**, *115*, 5604.
- (41) Tan, H. S.; Piletic, I. R.; Fayer, M. D. *J. Chem. Phys.* **2005**, *122*, 174501.
- (42) Rezus, Y. L. A.; Bakker, H. J. *J. Chem. Phys.* **2005**, *123*, 114502.
- (43) $\pi^* \leftarrow \pi^*$ absorption heralding the bpy-localized ³MLCT; a feature expected to diminish as some population transfers to the ³MC.